Preprints of the 21st IFAC World Congress (Virtual)
Berlin, Germany, July 12-17, 2020

Cooperative Navigation Based on Bearing and Range Measurements to Different Vehicles

David Santos * **and Pedro Batista** **

* *Institute for Systems and Robotics, Laboratory for Robotics and Engineering Systems, Lisboa, Portugal. (e-mail: david.dos.santos@tecnico.ulisboa.pt)*
** *Institute for Systems and Robotics, LARSyS, Instituto Superior Técnico, Universidade de Lisboa, Portugal. (email: pbatista@isr.tecnico.ulisboa.pt)*

Abstract: This paper presents a navigation solution for a vehicle operating in cooperation with two other. The vehicle is assumed to measure bearing to one of the aiding vehicles and range to the other. An observer with globally exponentially stable error dynamics is designed by obtaining an equivalent observable linear time-varying system using an artificial output and state augmentation. The observer relies on local measurements, as well as limited communication between the vehicles. Simulations are performed to assess the proposed solution.

Keywords: Navigation, bearing, range, cooperative navigation, Kalman filter.

1. INTRODUCTION

One fundamental component of autonomous vehicles is a navigation system capable of providing location in the operation area. While in most cases the Global Positioning System (GPS) is available, in underwater scenarios, due to electromagnetic signal attenuation, alternatives must be found. The simplest approach is the development of an Inertial Navigation System, as done in [1]. However, this method suffers from open loop integration of sensors' noise and bias, which, if used for a long time, may lead to significant errors.

Acoustic waves propagate well and with known velocity underwater, thus can be used to develop more sophisticated solutions. There are three broad classes of acoustic positioning systems: Long Baseline (LBL), Short Baseline (SBL), and Ultra-short Baseline (USBL) systems. Both the LBL and SBL systems use the travel time of acoustic waves to measure distances, from which it is possible to design observers capable of computing the vehicles location. Examples of the design of LBL systems can be seen in [2] and in [3]. In [4] an SBL system is designed. Alternatively, a USBL system not only uses the travel time of the signal to measure the distance but also uses phase differencing to measure the bearing to the signal emitter. One example of the design and implementation of such can be consulted in [5].

The systems presented before use acoustic signals to measure range and, in the case of USBL, bearing to emitters with known location. The position of the emitters needs not to be fixed, see for instance [6], where a system uses range measurements to floating buoys to determine its own position.

It is also possible to develop navigation systems based only on bearing measurements. In [7], observability requirements for 3-D tracking using angle measurements were studied. In [8–10], different solutions for bearing-only tracking were proposed.

Both the bearing and range measurements depend nonlinearly on the position of the vehicle, thus leading to nonlinear dynamic systems. Most solutions proposed to tackle this problem use observers such as, for example, the extended Kalman filter (EKF). However, such solutions lack guarantees of convergence. To deal with these non-linearities, it is also possible to find equivalent linear systems with the help of state augmentation and artificial outputs, as introduced in [11–13] for range-based localization and navigation systems, or in [14–16] for bearing-based systems.

In this paper, a navigation system for a vehicle moving underwater is designed. Two measurements are assumed to be available: i) bearing to one vehicle; and ii) range to a different vehicle. Besides, the positions of both aiding vehicles are assumed to be known. The bearing and range measurements make the considered system nonlinear, which means that a linear Kalman filter cannot be directly applied. To cope with this, state augmentation is performed and an artificial output is added, resulting in a linear system. The observability of the new system is studied in detail and observability conditions are derived. Alternatively, an algebraic solution for the vehicle position, only available in some scenarios, is derived, leading to an alternate linear system that can be used to complement

⋆ This work was supported by the Fundação para a Ciência e a Tecnologia (FCT) through LARSyS - FCT Plurianual funding 2020-2023 and through the FCT project DECENTER [LISBOA-01-0145-FEDER-029605], funded by the Programa Operacional Regional de Lisboa 2020 and PIDDAC programs.

the previous one, as the availability conditions of both are different. Finally, simulation results are presented to show the convergent behaviour of the proposed solution.

2. PROBLEM STATEMENT

Consider a formation of 3 vehicles, indexed from 1 to 3. All the vehicles are evolving in a fluid whose velocity is assumed to be constant. It is also assumed that the inertial positions, expressed in a local inertial frame, $\{I\}$, of vehicles 1 and 2 are known, provided by, for example, GPS or a long baseline system. The positions of each vehicle, expressed in $\{I\}$, are denoted by $\mathbf{p}_r(t) \in \mathbb{R}^3$, $\mathbf{p}_b(t) \in \mathbb{R}^3$, and $\mathbf{p}(t) \in \mathbb{R}^3$ for vehicles 1, 2, and 3, respectively. The velocity of the fluid, also expressed in $\{I\}$, is denoted by $\mathbf{v}_f(t) \in \mathbb{R}^3$.

Since the positions of vehicles 1 and 2 are known, the goal of this work is to design a navigation system for vehicle 3. As so, the nature of the sensors and measurements available to vehicles 1 and 2 is not relevant.

Vehicle 3 is moving with a velocity relative to the fluid, measured by a relative velocity sensor, such as a Doppler velocity log (DVL), and denoted by $\mathbf{v}(t) \in \mathbb{R}^3$, expressed in the body frame, $\{B\}$. This vehicle is also equipped with an attitude and heading reference system (AHRS), which provides the rotation matrix, $\mathbf{R}(t) \in SO(3)$, from $\{B\}$ to $\{I\}$.

The kinematics of vehicle 3 are given by

$$\begin{cases} \dot{\mathbf{p}}(t) = \mathbf{v}_f(t) + \mathbf{R}(t)\mathbf{v}(t) \\ \dot{\mathbf{v}}_f(t) = \mathbf{0} \end{cases}.$$

Vehicle 3 measures the range and bearing to vehicles 1 and 2, respectively, in discrete-time, as given by

$$\begin{cases} r(k) = \|\mathbf{p}_r(t_k) - \mathbf{p}(t_k)\| \\ \mathbf{d}(k) = \mathbf{R}^T(t_k)\dfrac{\mathbf{p}_b(t_k) - \mathbf{p}(t_k)}{\|\mathbf{p}_b(t_k) - \mathbf{p}(t_k)\|} \end{cases}.$$

Besides, it has access to the true positions of vehicles 1 and 2, which are known and communicated by those vehicles.

From now on, and unless specified otherwise, it is considered

$$\mathbf{d}(k) = \frac{\mathbf{p}_b(t_k) - \mathbf{p}(t_k)}{\|\mathbf{p}_b(t_k) - \mathbf{p}(t_k)\|}, \tag{1}$$

since this simplifies the computations. This is done without loss of generality since the matrix $\mathbf{R}(t_k)$ is available and invertible. For simulation purposes, the original bearing measurement is used.

Because the communications, bearings, and range measurements between vehicles are only available at a frequency too low for the system to be studied as time-continuous, the system must be discretized, which leads to

$$\begin{cases} \mathbf{p}(t_{k+1}) = \mathbf{p}(t_k) + T\mathbf{v}_f(t_k) + \mathbf{u}(k) \\ \mathbf{v}_f(t_{k+1}) = \mathbf{v}_f(t_k) \\ r(k) = \|\mathbf{p}_r(t_k) - \mathbf{p}(t_k)\| \\ \mathbf{d}(k) = \dfrac{\mathbf{p}_b(t_k) - \mathbf{p}(t_k)}{\|\mathbf{p}_b(t_k) - \mathbf{p}(t_k)\|} \end{cases}, \tag{2}$$

where T is the sampling period and $\mathbf{u}(k)$ is given by

$$\mathbf{u}(k) = \int_{t_k}^{t_{k+1}} \mathbf{R}(t)\mathbf{v}(t)dt. \tag{3}$$

The problem addressed in this paper is that of designing an observer, with globally exponentially stable (GES) error dynamics, for the position and local fluid velocity of vehicle 3, $\mathbf{p}(t_k)$ and $\mathbf{v}_f(t_k)$, respectively. This is done by finding an equivalent observable linear system, for which a Kalman filter is designed.

3. OBSERVER DESIGN

The dynamic system (2) is nonlinear due to the bearing and range outputs. To address the first non-linearity, the bearing output is replaced by a linear artificial one. To address the second non-linearity, state augmentation is applied.

3.1 Artificial output

First, note that

$$\mathbf{d}(k)\mathbf{d}^T(k)\mathbf{d}(k) = \mathbf{d}(k)$$

since $\mathbf{d}(k)$ is a unit vector, from which it is possible to write

$$(\mathbf{I} - \mathbf{d}(k)\mathbf{d}^T(k))\mathbf{d}(k) = \mathbf{0}. \tag{4}$$

Combining (1) with (4) gives

$$(\mathbf{I} - \mathbf{d}(k)\mathbf{d}^T(k))\mathbf{p}_b(t_k) = (\mathbf{I} - \mathbf{d}(k)\mathbf{d}^T(k))\mathbf{p}(t_k). \tag{5}$$

Since all the terms in the left-hand side of (5) are known, it is possible to define the artificial output

$$\mathbf{z}(k) \coloneqq (\mathbf{I} - \mathbf{d}(k)\mathbf{d}^T(k))\mathbf{p}(t_k) \in \mathbb{R}^3.$$

Also, since $\mathbf{d}(k)$ is known, $\mathbf{z}(k)$ is linear on the state $\mathbf{p}(t_k)$. Replacing $\mathbf{d}(k)$ by $\mathbf{z}(k)$ in (2) yields

$$\begin{cases} \mathbf{p}(t_{k+1}) = \mathbf{p}(t_k) + T\mathbf{v}_f(t_k) + \mathbf{u}(k) \\ \mathbf{v}_f(t_{k+1}) = \mathbf{v}_f(t_k) \\ \mathbf{z}(k) = (\mathbf{I} - \mathbf{d}(k)\mathbf{d}^T(k))\mathbf{p}(t_k) \\ r(k) = \|\mathbf{p}_r(t_k) - \mathbf{p}(t_k)\| \end{cases}. \tag{6}$$

3.2 System augmentation

Define as states

$$\begin{cases} \mathbf{x}_1(k) \coloneqq \mathbf{p}(t_k) \\ \mathbf{x}_2(k) \coloneqq \mathbf{v}_f(t_k) \end{cases}.$$

The dynamic system (6) is still nonlinear due to the range measurement. A linear system is obtained by adding a state

$$x_3(k) \coloneqq \|\mathbf{p}_r(t_k) - \mathbf{p}(t_k)\|.$$

The evolution of $x_3(k)$ is obtained by expanding

$$r^2(k+1) = \|\mathbf{p}_r(t_{k+1}) - \mathbf{p}(t_{k+1})\|^2$$

using (6), which gives

$$\begin{aligned} r^2(k+1) = \; & 2(\mathbf{u}(k) - \Delta\mathbf{p}_r(t_k))^T\mathbf{p}(t_k) \\ & + 2T(\mathbf{u}(k) - \mathbf{p}_r(t_{k+1}))^T\mathbf{v}_f(t_k) + r^2(k) \\ & + 2T\mathbf{p}^T(t_k)\mathbf{v}_f(t_k) + T^2\|\mathbf{v}_f(t_k)\|^2 \\ & + \|\mathbf{p}_r(t_{k+1}) - \mathbf{u}(k)\|^2 - \|\mathbf{p}_r(t_k)\|^2, \end{aligned} \tag{7}$$

where $\Delta\mathbf{p}_r(t_k) \coloneqq \mathbf{p}_r(t_{k+1}) - \mathbf{p}_r(t_k)$. Adding the states

$$\begin{cases} x_4(k) \coloneqq \mathbf{p}^T(t_k)\mathbf{v}_f(t_k) \\ x_5(k) \coloneqq \|\mathbf{v}_f(t_k)\|^2 \end{cases}$$

and noting that $r^2(k) = r(k)x_3(k)$ allows to rewrite (7) as

$$\begin{aligned} x_3(k+1) = \; & \frac{2}{r(k+1)}(\mathbf{u}(k) - \Delta\mathbf{p}_r(t_k))^T\mathbf{x}_1(k) \\ & + \frac{2T}{r(k+1)}(\mathbf{u}(k) - \mathbf{p}_r(t_{k+1}))^T\mathbf{x}_2(k) \\ & + \frac{r(k)}{r(k+1)}x_3(k) + \frac{2T}{r(k+1)}x_4(k) \\ & + \frac{T^2}{r(k+1)}x_5(k) \\ & + \frac{\|\mathbf{p}_r(t_{k+1}) - \mathbf{u}(k)\|^2 - \|\mathbf{p}_r(t_k)\|^2}{r(k+1)}. \end{aligned}$$

The evolution of the new states $x_4(k)$ and $x_5(k)$ is simply obtained using (2), as given by

$$\begin{cases} x_4(k+1) = \mathbf{u}^T(k)\mathbf{x}_2(k) + x_4(k) + Tx_5(k) \\ x_5(k+1) = x_5(k) \end{cases}.$$

Defining the augmented state vector

$$\mathbf{x}(k) \coloneqq \begin{bmatrix} \mathbf{x}_1(k) \\ \mathbf{x}_2(k) \\ x_3(k) \\ x_4(k) \\ x_5(k) \end{bmatrix} \in \mathbb{R}^9$$

and the output vector

$$\mathbf{y}(k) \coloneqq \begin{bmatrix} \mathbf{z}(k) \\ r(k) \end{bmatrix} \in \mathbb{R}^4$$

leads to a linear time-varying system (LTV), which can be written as

$$\begin{cases} \mathbf{x}(k+1) = \boldsymbol{\mathcal{A}}_k\mathbf{x}(k) + \boldsymbol{\mathcal{B}}_k\mathbf{u}^*(k) \\ \mathbf{y}(k) = \boldsymbol{\mathcal{C}}_k\mathbf{x}(k) \end{cases}. \tag{8}$$

The system matrices are given by

$$\boldsymbol{\mathcal{A}}_k = \left[\begin{array}{cccc|c} \mathbf{I}_3 & T\mathbf{I}_3 & \mathbf{0} & \mathbf{0} & \mathbf{0} \\ \mathbf{0} & \mathbf{I}_3 & \mathbf{0} & \mathbf{0} & \mathbf{0} \\ \hline & & \boldsymbol{\mathcal{A}}_k^{(3)} & & \\ \hline \mathbf{0} & \mathbf{u}^T(k) & 0 & 1 & T \\ \mathbf{0} & \mathbf{0} & 0 & 0 & 1 \end{array}\right] \in \mathbb{R}^{9\times 9},$$

where

$$\boldsymbol{\mathcal{A}}_k^{(3)} = \frac{1}{r(k+1)}\begin{bmatrix} 2(\mathbf{u}(k) - \Delta\mathbf{p}_r(t_k)) \\ 2T(\mathbf{u}(k) - \mathbf{p}_r(t_{k+1})) \\ r(k) \\ 2T \\ T^2 \end{bmatrix}^T \in \mathbb{R}^{1\times 9},$$

$$\boldsymbol{\mathcal{B}}_k = \begin{bmatrix} \mathbf{I}_3 & \mathbf{0} \\ \mathbf{0} & \mathbf{0} \\ \mathbf{0} & 1 \\ \mathbf{0} & 0 \\ \mathbf{0} & 0 \end{bmatrix} \in \mathbb{R}^{9\times 4},$$

$$\mathbf{u}^*(k) = \begin{bmatrix} \mathbf{u}(k) \\ \dfrac{\|\mathbf{p}_r(t_{k+1}) - \mathbf{u}(k)\|^2 - \|\mathbf{p}_r(t_k)\|^2}{r(k+1)} \end{bmatrix} \in \mathbb{R}^4,$$

and

$$\boldsymbol{\mathcal{C}}_k = \begin{bmatrix} \boldsymbol{\mathcal{C}}_k^{(1)} \\ \boldsymbol{\mathcal{C}}_k^{(2)} \end{bmatrix} = \begin{bmatrix} \mathbf{I}_3 - \mathbf{d}(k)\mathbf{d}^T(k) & \mathbf{0} & \mathbf{0} & \mathbf{0} & \mathbf{0} \\ \mathbf{0} & & \mathbf{0} & 1 & 0 & 0 \end{bmatrix} \in \mathbb{R}^{4\times 9}.$$

3.3 Observability

Define

$$\Delta^i\mathbf{p}_r(t_k) \coloneqq \mathbf{p}_r(t_{k+i}) - \mathbf{p}_r(t_k)$$

and

$$\mathbf{u}^i(k) \coloneqq \sum_{j=k}^{k+i-1}\mathbf{u}(j).$$

The following theorem addresses the observability of the linear system (8). For the sake of easiness of notation, let $\mathbf{d}_k \coloneqq \mathbf{d}(k)$ be used indifferently throughout the paper.

Theorem 1. *If* $\operatorname{rank}(\mathbf{M}_{N-1}) = 8$*, where*

$$\mathbf{M}_i \coloneqq \left[\begin{array}{c|cc} \mathbf{M}_i^{(1)} & \begin{matrix}1 & 1\\ 2 & 4\\ \vdots & \vdots \\ i & i^2\end{matrix} \\ \hline \mathbf{M}_i^{(2)} & \mathbf{0} \end{array}\right] \in \mathbb{R}^{(2i+1)\times 8},$$

with

$$\mathbf{M}_i^{(1)} \coloneqq \begin{bmatrix} \big(\mathbf{u}(k_0) - \Delta\mathbf{p}_r(t_{k_0})\big)^T & \big(\mathbf{u}(k_0) - \mathbf{p}_r(t_{k_0+1})\big)^T \\ \big(\mathbf{u}^2(k_0) - \Delta^2\mathbf{p}_r(t_{k_0})\big)^T & 2\big(\mathbf{u}^2(k_0) - \mathbf{p}_r(t_{k_0+2})\big)^T \\ \vdots & \vdots \\ \big(\mathbf{u}^i(k_0) - \Delta^i\mathbf{p}_r(t_{k_0})\big)^T & i\big(\mathbf{u}^i(k_0) - \mathbf{p}_r(t_{k_0+i})\big)^T \end{bmatrix}$$

and

$$\mathbf{M}_i^{(2)} \coloneqq \begin{bmatrix} \mathbf{I} - \mathbf{d}_{k_0}\mathbf{d}_{k_0}^T & \mathbf{0} \\ \mathbf{I} - \mathbf{d}_{k_0+1}\mathbf{d}_{k_0+1}^T & \mathbf{I} - \mathbf{d}_{k_0+1}\mathbf{d}_{k_0+1}^T \\ \vdots & \vdots \\ \mathbf{I} - \mathbf{d}_{k_0+i}\mathbf{d}_{k_0+i}^T & i\big(\mathbf{I} - \mathbf{d}_{k_0+i}\mathbf{d}_{k_0+i}^T\big) \end{bmatrix},$$

then the system (8) is observable on the interval $[k_0, k_0 + N]$.

The proof is not presented due to space limitations. The theorem takes the observability matrix of the system and simplifies it to one of easier understanding. Still, it is not possible to draw simple conclusions of geometric interpretation relative to the system's observability. The system needs excitation to be observable, however this need is less demanding than when only one bearing or one range are available. It is possible that neither the system with one bearing nor the the system with one range are observable but this one is.

Theorem 1 addresses the observability of the linear augmented system (8), however, there is no guarantee of observability for the original nonlinear system (2). The following theorem addresses this issue.

Theorem 2. *If* $\operatorname{rank}(\mathbf{M}_{N-1}) = 8$*, then the system (2) is observable on* $[k_0, k_0 + N]$*. Furthermore, the initial conditions of (2) and (8) match.*

The proof of this theorem is not presented due to space limitations.

With the observability studied, the design of a Kalman filter for (8) leads to an observer with guarantees of GES error dynamics for (2). The design of a Kalman filter is the obvious choice since it is applied to a system that is linear in the state. This is due to the fact that $\mathbf{d}(k)$ is known. The Kalman filter yields globally exponentially stable error dynamics if the system is shown to be uniformly completely observable [17]. Here, only observability was shown due to space limitations but the proof of uniform complete observability, while tedious, follows similar steps considering uniform bounds in time.

4. ALGEBRAIC SOLUTION

In the previous section, an LTV system and its observability conditions were derived. When this system is observable, it can be used to estimate the state of system (2). However, it is possible that the original system (2) is observable but the LTV system (8) is not. This is evidenced in the following theorem.

Theorem 3. *If* $\|\mathbf{p}_r(t_k)-\mathbf{p}_b(t_k)\| < r(k)$ *for* $k = k_0, k_0+1$, *then the system (2) is observable on the interval* $[k_0, k_0+2]$.

Proof. From (1) it is possible to write

$$\mathbf{p}(t_k) = \mathbf{p}_b(t_k) - \|\mathbf{p}_b(t_k) - \mathbf{p}(t_k)\|\mathbf{d}(k), \tag{9}$$

which can be used to conclude that

$$\begin{aligned} r^2(k) =& \|\mathbf{p}_r(t_k) - \mathbf{p}(t_k)\|^2 \\ =& \big\|\mathbf{p}_r(t_k) - \mathbf{p}_b(t_k) + \|\mathbf{p}_b(t_k) - \mathbf{p}(t_k)\|\mathbf{d}(k)\big\|^2. \end{aligned}$$

The previous equation can be expanded into a quadratic equation on $\|\mathbf{p}_b(t_k) - \mathbf{p}(t_k)\|$, which, under the assumptions of the theorem, will have one positive and one negative solutions. Since only the positive solution is feasible for a distance, it is possible to determine $\|\mathbf{p}_b(t_k) - \mathbf{p}(t_k)\|$.

It is now possible to determine $\mathbf{p}(t_{k_0})$ and $\mathbf{p}(t_{k_0+1})$ using (9). Finally, $\mathbf{v}_f(t_{k_0})$ is given by

$$\mathbf{v}_f(t_{k_0}) = \frac{\mathbf{p}(t_{k_0+1}) - \mathbf{p}(t_{k_0}) - \mathbf{u}(k_0)}{T}.$$

As so, the initial state of the system in uniquely determined by the input and output of the system at instants k_0 and $k_0 + 1$, concluding the proof of the theorem. □

This theorem can be used to design a Kalman filter for

$$\begin{cases} \mathbf{p}(t_{k+1}) = \mathbf{p}(t_k) + T\mathbf{v}_f(t_k) + \mathbf{u}(k) \\ \mathbf{v}_f(t_{k+1}) = \mathbf{v}_f(t_k) \\ \mathbf{p}(t_{k+1}) = \mathbf{p}_b(t_k) - \|\mathbf{p}_b(t_k) - \mathbf{p}(t_k)\|\mathbf{d}(k) \end{cases}, \tag{10}$$

with

$$\|\mathbf{p}_b(t_k) - \mathbf{p}(t_k)\| = \frac{-b(k) + \sqrt{b^2(k) - 4c(k)}}{2}$$

and

$$\begin{cases} b(k) = 2(\mathbf{p}_r(t_k) - \mathbf{p}_b(t_k))^T\mathbf{d}(k) \\ c(k) = \|\mathbf{p}_r(t_k) - \mathbf{p}_b(t_k)\|^2 - r^2(k) \end{cases}.$$

5. SIMULATION RESULTS

Simulations are presented in this section to illustrate the behaviour of the proposed solutions when the measurements are subject to noise.

5.1 Setup

To perform the simulations, a sampling period of 1s is assumed for the bearing and range measurements and the communications between the vehicles, while all the other measurements are assumed to be available at 100Hz. Azimuth and inclination are measured, from which the bearing is obtained as

$$\mathbf{d} = \begin{bmatrix} \sin(\theta)\cos(\phi) \\ \sin(\theta)\sin(\phi) \\ \cos(\theta) \end{bmatrix},$$

where ϕ and θ are, respectively, the azimuth and inclination angles to the other vehicle. Zero-mean white gaussian noise with a standard deviation of 1° was added to both angles. For vehicles 1 and 2, the position is available but zero-mean white gaussian noise was added with a standard deviation of 0.1m in each component. Some correlation was added, resulting in the covariance matrix

$$0.01 \times \begin{bmatrix} 1 & 0.1 & 0.1 \\ 0.1 & 1 & 0.1 \\ 0.1 & 0.1 & 1 \end{bmatrix}.$$

For the Euler angles, used to obtain the rotation matrix, uncorrelated zero-mean white Gaussian noise was added with a standard deviation of 0.01° for the pitch and roll angles and 0.03° for the yaw angle. The relative velocity to the fluid was corrupted by uncorrelated zero-mean white Gaussian noise with standard deviation of 0.01 m/s. Finally, the range measurement was corrupted by additive zero-mean white Gaussian noise with a standard deviation of 0.1 m. The integral in (3) was computed using the trapezoidal rule. The fluid velocity was set to $\mathbf{v}_f = [0.2\ 0.3\ 0.15]^T$ m/s.

Two different scenarios were considered: i) when the augmented system is observable; ii) when the algebraic solution is valid. In both cases, the vehicles performed the same type of trajectory with different starting points. The trajectories were generated with way points, which are described in Table 1. The differences between the cases are the initial positions and the enrichment of the trajectory of vehicle 1. The starting points are described in Table 2. The acceleration was limited to 0.01 m/s^2, which resulted in the curve presented in Fig. 1. In scenario i), the trajectory for vehicle 1 was enriched by adding $10\sin(0.1t)[1\ 1\ 1]^T$ to its position.

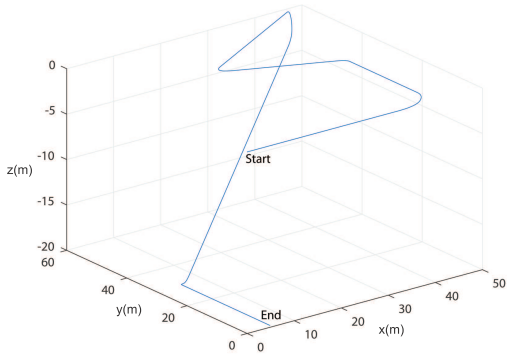

Fig. 1. Trajectory curve

Time (s)	Position (m)
0	[0 0 0]
100	[40 0 0]
200	[40 20 0]
300	[40 30 0]
400	[20 40 0]
600	[50 60 0]
800	[5 30 -20]
1000	[5 0 -20]

Table 1. Trajectory waypoints for vehicle 1

5.2 Simulation Results

To assess the performance of the proposed solution, simulations were performed for both scenarios. In scenario i), a

Vehicle	Initial Position (m)	
	i)	ii)
1	[0 0 0]	[0 0 0]
2	[100 100 0]	[100 100 0]
3	[70 70 -40]	[130 130 -40]

Table 2. Initial positions.

linear Kalman filter is applied to (8), while in scenario ii) a linear Kalman filter is applied to (10) instead. In scenario i), the state covariance matrix was set to

$$\mathbf{Q} = \text{diag}(0.01\mathbf{I}, 0.000005\mathbf{I}, 10^{-8}, 10^{-10}, 10^{-8}).$$

In scenario ii), it was set to $\text{diag}(0.01\mathbf{I}, 0.000005\mathbf{I})$. The output covariance matrices were set to $\text{diag}(50\mathbf{I}, 1)$ and $\mathbf{I}$, for scenario i) and ii), respectively. The initial estimates for both scenarios were drawn from a Gaussian centred in the true state and with covariance matrix $\mathbf{P} = \text{diag}(10^2\mathbf{I}_3, \mathbf{I}_6)$.

The estimation error in transient state can be seen in Fig. 2 and Fig. 3 for scenario i) and Fig. 4 and Fig. 5 for scenario ii). It is possible to see that the convergence in scenario ii) is faster, as expected, since the position is directly available.

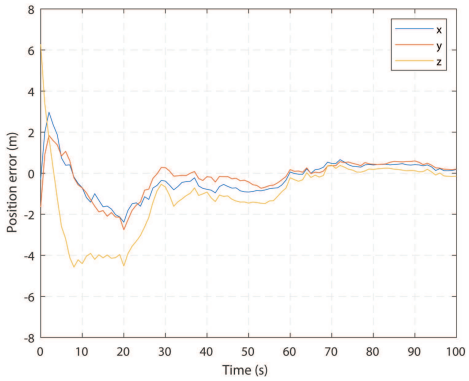

Fig. 2. Scenario i) Error of position estimates

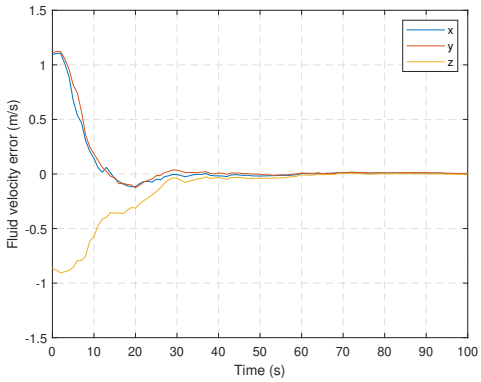

Fig. 3. Scenario i) Error of fluid velocity estimates

The estimation error in steady state can be seen in Fig. 6 and Fig. 7 for scenario i) and Fig. 8 and Fig. 9 for scenario ii). It is possible to see that in scenario i) the estimates present lower error in steady-state.

It is important to note that the two scenarios have different conditions and that it is not useful nor important to compare the performance between the two options. Instead, it would be more relevant to compare the performance of these two solutions with the performance of the extended

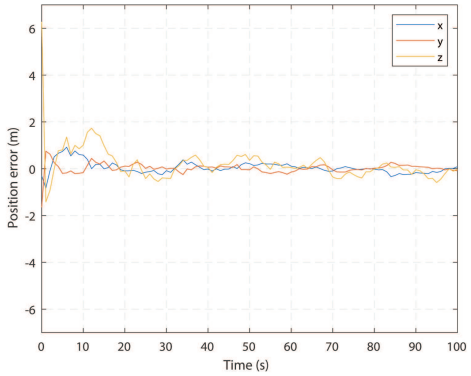

Fig. 4. Scenario ii) Error of the position estimates

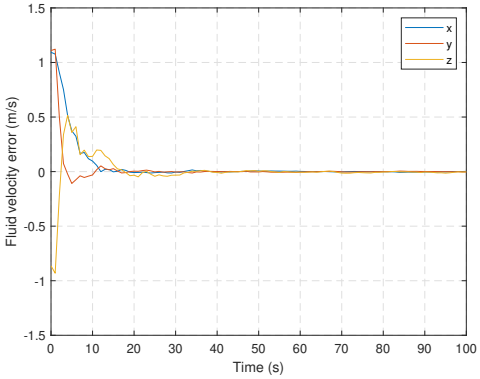

Fig. 5. Scenario ii) Error of the fluid velocity estimates

Kalman filter or the unscented Kalman filter, which will be done in future work.

6. CONCLUSIONS

In underwater scenarios the communication bandwidth is very limited, rendering centralized navigation solutions impossible to implement. This paper presents a cooperative, decentralized navigation solution for formations of underwater vehicles where one bearing and one range to different vehicles are available. In order to cope with the nonlinear nature of the outputs, artificial outputs and state augmentation are employed that render the dynamics linear, thus allowing for the design of a Kalman filter with GES errors dynamics. In some circumstances, it is possible to determine an algebraic solution. Finally, simulation results were presented to assess the behaviour of the proposed solutions.

REFERENCES

[1] B. Barshan and H. Durrant-Whyte, *"Inertial navigation systems for mobile robots"*, IEEE Transactions on Robotics and Automation, vol. 11, pp. 328–342, jun 1995.

[2] L. Techy, K. A. Morgansen, and C. A. Woolsey, *"Long-baseline acoustic localization of the Seaglider underwater glider"*, in Proceedings of the 2011 American Control Conference, pp. 3990–3995, IEEE, jun 2011.

[3] L. L. Whitcomb, D. R. Yoerger, and H. Singh, *"Combined Doppler / LBL Based Navigation of Underwater Vehicles 1 Introduction"*, 11th International Symposium on Unmanned Untethered Submersible Technology, no. 10015, 1999.

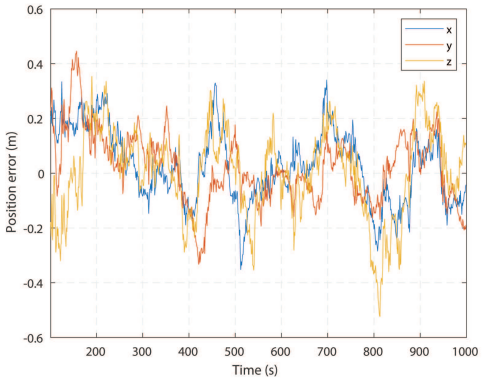

Fig. 6. Scenario i) Error of the position estimates

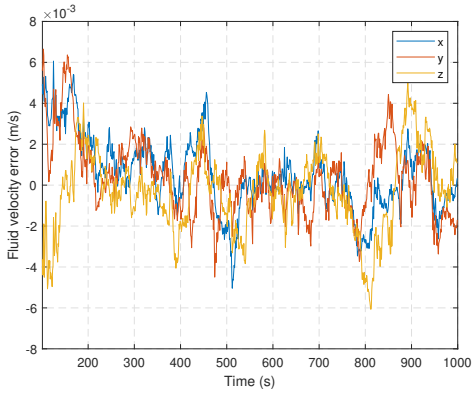

Fig. 7. Scenario i) Error of the fluid velocity estimates

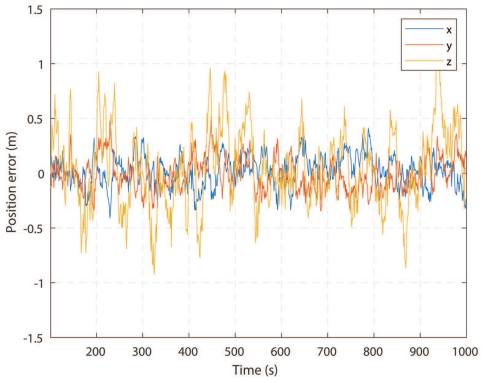

Fig. 8. Scenario ii) Error of the position estimates

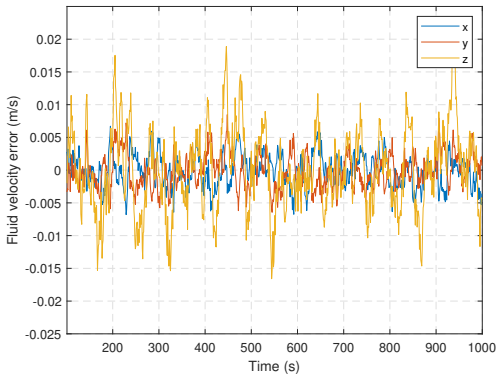

Fig. 9. Scenario ii) Error of the fluid velocity estimates

[4] S. Smith and D. Kronen, *"Experimental results of an inexpensive short baseline acoustic positioning system for AUV navigation"*, in Oceans '97. MTS/IEEE Conference Proceedings, vol. 1, pp. 714– 720, IEEE, oct 1997.

[5] J. Reis, M. Morgado, P. Batista, P. Oliveira, and C. Silvestre, *"Design and Experimental Validation of a USBL Underwater Acoustic Positioning System"*, Sensors, vol. 16, p. 1491, sep 2016.

[6] H. Thomas, *"GIB buoys: an interface between space and depths of the oceans"*, in Proceedings of the 1998 Workshop on Autonomous Underwater Vehicles (Cat. No.98CH36290), pp. 181–184, IEEE, aug 1998.

[7] S. Hammel and V. Aidala, *"Observability Requirements for Three-Dimensional Tracking via Angle Measurements"*, IEEE Transactions on Aerospace and Electronic Systems, vol. AES-21, pp. 200– 207, mar 1985.

[8] J. Zhang and H. Ji, *"Distributed multi-sensor particle filter for bearings-only tracking"*, International Journal of Electronics, vol. 99, pp. 239–254, feb 2012.

[9] T. Brehard and J.-P. Le Cadre, *"Hierarchical particle filter for bearings-only tracking"*, IEEE Transactions on Aerospace and Electronic Systems, vol. 43, pp. 1567–1585, oct 2007.

[10] K. Lakshmi Prasanna, S. Koteswara Rao, S. B. Karishma, and A. Jawahar, *"Application of Cubature Kalman Filter for Bearings only Target Tracking"*, Indian Journal of Science and Technology, vol. 9, may 2016.

[11] P. Batista, C. Silvestre, and P. Oliveira, *"GES Source Localization based on Discrete-Time Position and Single Range Measurements"*, in 21st Mediterranean Conference on Control & Automation, pp. 1248–1253, 2013.

[12] P. Batista, *"GES Long Baseline Navigation With Unknown Sound Velocity and Discrete-Time Range Measurements"*, IEEE Transactions on Control Systems Technology, vol. 23, pp. 219–230, jan 2015.

[13] D. Viegas, P. Batista, P. Oliveira, and C. Silvestre, *"Decentralized state observers for range-based position and velocity estimation in acyclic formations with fixed topologies"*, International Journal of Robust and Nonlinear Control, vol. 26, pp. 963–994, mar 2016

[14] P. Batista, C. Silvestre, and P. Oliveira, *"Globally exponentially stable filters for source localization and navigation aided by direction measurements"*, Systems and Control Letters, vol. 62, no. 11, pp. 1065–1072, 2013.

[15] P. Batista, C. Silvestre, and P. Oliveira, *"GES source localization and navigation based on discrete-time bearing measurements"*, Proceedings of the IEEE Conference on Decision and Control, no. 3, pp. 5066–5071, 2013.

[16] P. Batista, C. Silvestre, and P. Oliveira, *"Navigation systems based on multiple bearing measurements"*, IEEE Transactions on Aerospace and Electronic Systems, vol. 51, no. 4, pp. 2887–2899, 2015.

[17] A. Jazwinski, *"Stochastic Processes and Filtering Theory"*, Academic Press, Inc., 1970.